Impact of disorder outside the CuO_2 planes of electron-doped superconductors: Different effect on localization and T_c between Gd and Sm doping

Chenghai Sun, Hongshun Yang,* Lu Cheng, Jianbin Wang, Xiangyi Xu, Shaoqing Ke, and Liezhao Cao
Department of Physics, University of Science and Technology of China, Hefei, Anhui 230026, People's Republic of China
(Received 11 June 2008; revised manuscript received 29 July 2008; published 18 September 2008)

The thermopower $S(T)$, Hall coefficient R_H, and resistivity $\rho(T)$ are studied for $Nd_{1.85-x}M_xCe_{0.15}CuO_{4\pm\delta}$ (M=Gd and Sm) single crystals. Disorder is introduced into the cation sites outside the CuO_2 planes in the two systems and its degree is controlled by changing M content. Such doping nominally does not change the doped carrier density, which is confirmed by R_H. $S(T)$ is analyzed in terms of a semiempirical model above 120 K for both doping, which assumes the coexistence of a narrow electron band and a broad one. In this model, both the bandwidth for the density of states and the bandwidth of the effective conductivity broaden with increasing x for both doping, while the tendency for localization is increased for Gd doping but nearly unchanged for Sm doping, which could be understood by stronger electronic disorder for Gd doping than that for Sm doping. This may be resulted from the difference in ionic radius ($Gd^{3+}<Sm^{3+}<Nd^{3+}$). Furthermore, for Gd doping the superconducting T_c is strongly depressed with increasing the doping concentration, while for Sm doping T_c is nearly unchanged with increasing Sm content, which implies that the superconducting T_c may be related to the localization and the band structure of the itinerant carriers.

DOI: 10.1103/PhysRevB.78.104518 PACS number(s): 74.62.Dh, 74.25.Fy, 72.15.Rn

I. INTRODUCTION

High-temperature superconductivity is achieved upon doping charge carriers into the CuO_2 planes in copper oxide materials. Doping is made, in most cases, by chemical substitution or removing oxygen atoms, which inevitably introduces disorder into the building blocks between the CuO_2 planes.[1,2] The impact of such disorder on the electronic structure and the superconducting properties of high-T_c cuprates is still poorly understood. Since T_c is so strongly dependent on doping level, disorder appears to have a secondary effect. However, García-Muñoz *et al.*[3] demonstrated that T_c is systematically increased with increasing cell dimensions in the LO blocks in $L_{2-x-y}L'_yCe_xCuO_4$ (L, L'=La, Pr, Nd, Sm, and Gd) and that pressure always leads to a decrease in the in-plane electron density. They ascribed T_c reduction to the intrinsic dependence on the interatomic distances possibly related to a distorted structure. Moreover, it is noticed that many models are proposed to describe the normal-state properties of cuprates, such as charge stripes,[4] and the modified two-dimensional (2D) single-carrier Fermi-liquid model.[5] All these models assume a strong electron-electron and/or electron-phonon interaction. The disorder introduced by cationic or oxygen removing influences the spectrum of excitations, making the physics of the system more complex. Problems that have been discussed at present are the relevance of disorder to localization and localization to superconductivity as well as the model which could describe the normal-state properties of high-T_c superconductors appropriately.

As a powerful way to study the nature of the charge transport, thermopower (S), which is sensitive to details of the Fermi surface and band structure, has been extensively studied in different series of high-T_c copper oxides. This is reflected in a large number of investigations of different alloy systems, such as $L_{2-x}Ce_xCuO_4$ (L=La, Nd, Pr, and so on)[6–8] as well as the holelike compounds.[9–19] These studies have revealed trends for the magnitude of S and for the temperature and doping concentration dependences. Especially for the hole-doped compounds, one important result is the useful empirical relation between the hole concentration p in the planes and the magnitude of S at room temperature.[20] In general, for semiconducting or insulating materials with low carrier concentration, S is positive and large and decreases with increasing carrier number. For metallic samples, on the other hand, S is small and has a characteristic behavior for both underdoped and optimally doped samples at temperatures above the superconducting transition temperature T_c. For overdoped samples with a larger carrier density, S becomes positive for electron-doped compounds but negative for hole-doped ones. However, since the thermopower in near optimal-doped samples is very small with the order of 1 μV, about tens times smaller than that in hole-doped cuprates,[21] the high-resolution thermopower data of the electron-doped superconductors were still lacking especially with different disorder degrees in the building blocks.

In the last few years, large efforts were devoted to study the impact of the disorder on the properties of the hole-doped superconductor, but few experiments were carried on the electron-doped one.[3,22] So we performed the thermopower, Hall-coefficient R_H, and resistivity experiments on $Nd_{1.85-x}M_xCe_{0.15}CuO_{4\pm\delta}$ (M=Gd and Sm) with the doping in the building block next to the CuO_2 planes. The motivation is to study the evolution of the thermopower with the doping and to investigate whether the thermopower could contribute to shed light on the origin of the depression of T_c. It is found that $S(T)$ could be described in terms of a semiempirical model above 120 K for both dopings, which assumes the existence of a narrow electron band. For Gd doping the superconducting T_c is strongly depressed with increasing doping concentration in spite of the fact that this doping nominally does not change the doped carrier density, while for Sm doping T_c is nearly unchanged with increasing Sm content, which indicates that the superconducting T_c may be related to the localization and the band structure of the itinerant carriers.

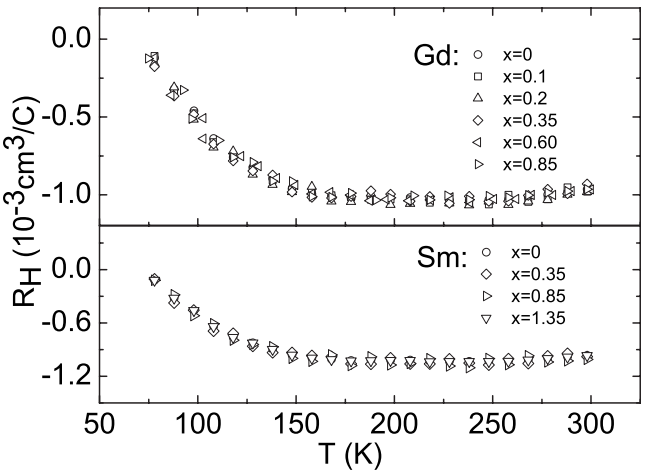

FIG. 1. The temperature dependence of the Hall coefficient for $Nd_{1.85-x}M_xCe_{0.15}CuO_{4\pm\delta}$ (M=Gd and Sm).

II. EXPERIMENTAL DETAILS

$Nd_{1.85-x}M_xCe_{0.15}CuO_{4\pm\delta}$ (M=Gd and Sm) single crystals (x=0, 0.1, 0.2, 0.35, 0.60, and 0.85 for Gd doping and x=0, 0.35, 0.85, and 1.35 for Sm doping) were grown by the self-flux method.[23] All the samples in each series were prepared to have the same doping level by fixing the Ce content, which was checked by the inductively coupled-plasma spectroscopy. The typical size of the single crystals is about $a \times b \times c = 3 \times 1 \times 0.1$ mm^3. To assure uniform oxygen distribution and same oxygen content, the samples were annealed under the same conditions at 900 °C for 24 h in flowing N_2 gas, and then the temperature is decreased to room temperature at a rate of 60 °C/h. In order to ensure whether such doping changes the doped carrier density, the constant carrier density was confirmed by measurement of the Hall coefficient (with current parallel to the planes and magnetic fields applied perpendicular to the planes) in the temperature range from 77 to 300 K. The result of which is shown in Fig. 1 for $Nd_{1.85-x}M_xCe_{0.15}CuO_{4\pm\delta}$. Both magnitude and temperature dependences of the Hall coefficient do not show significant change within experimental error, indicating that the normal-state carrier density is almost the same. X-ray diffraction was performed on the two series samples and no impurity reflections were observed in these samples.

ρ was measured by the standard four-probe method and S was performed using reversible temperature differences from 0.8 to 2 K. The crystal was mounted on the top of two well thermal-separated copper blocks. The temperature at the two ends of the crystal was controlled automatically within the precision of 0.004 K. Each data point was the average of 100 points and the error of the S measurement system was smaller than 0.1 μV/K. All the S data were corrected for the contribution of the Cu leads, which calibrated by pure Pb at high temperatures and by superconducting $YBa_2Cu_3O_{7-\delta}$ at low temperatures.

III. RESULTS AND ANALYSES

The temperature dependence of thermopower for $Nd_{1.85-x}M_xCe_{0.15}CuO_{4\pm\delta}$ (M=Gd and Sm) is shown in Fig. 2(a) for Gd-doped samples and in Fig. 2(b) for Sm-doped samples, respectively. As shown in Fig. 1(a), $S(T)$ is positive in the whole temperature range for x=0 sample. At high temperatures, $S(T)$ follows an almost linear temperature dependence and with decreasing temperature, two maxima, a broad one at about 170 K and the other sharp one slightly above the superconducting temperature T_c, are observed. Finally, it decreases rapidly to zero as T_c is approached. As the dopant concentration x is increased, the magnitude of the thermopower is decreased and eventually becomes negative in the whole temperature region up to x=0.85, while the temperature dependence of thermopower is nearly unchanged with an exception at x=0.85, where the strong localization is occurred especially in the low-temperature region just as demonstrated in Figs. 3(a) and 3(b). We notice that the temperature-dependent behaviors of the thermopower for x=0 at high temperatures are inconsistent with the results of $Nd_{1.85}Ce_{0.15}CuO_{4\pm\delta}$ at zero fields pointed out by Jiang *et al.* in Ref. 22. We think that these deviations may be resulted from the strong dependence of the thermopower on the annealing conditions just as mentioned in Ref. 22. At the same time, It must be emphasized that we tried to synthesize $Nd_{1.85-x}Gd_xCe_{0.15}CuO_{4\pm\delta}$ single crystals with $x>0.85$, but we failed to do so, which may be resulted from the solubility limit being reached. For the Sm-doped samples, the temperature dependence of thermopower is similar to that of Gd-doped samples. Especially, $S(T)$'s for

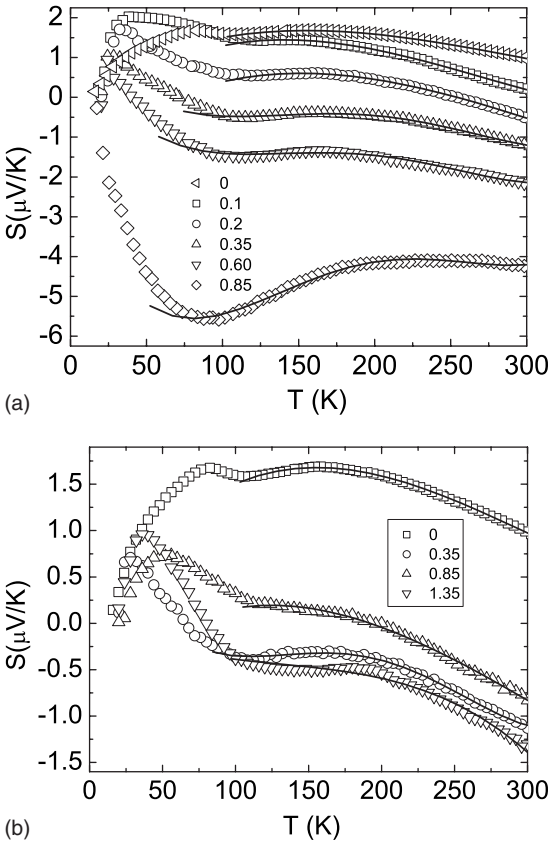

FIG. 2. The temperature dependence of thermopower S for (a) $Nd_{1.85-x}Gd_xCe_{0.15}CuO_{4\pm\delta}$ and (b) $Nd_{1.85-x}Sm_xCe_{0.15}CuO_{4\pm\delta}$ samples. The curves are fits to the model of Eq. (1).

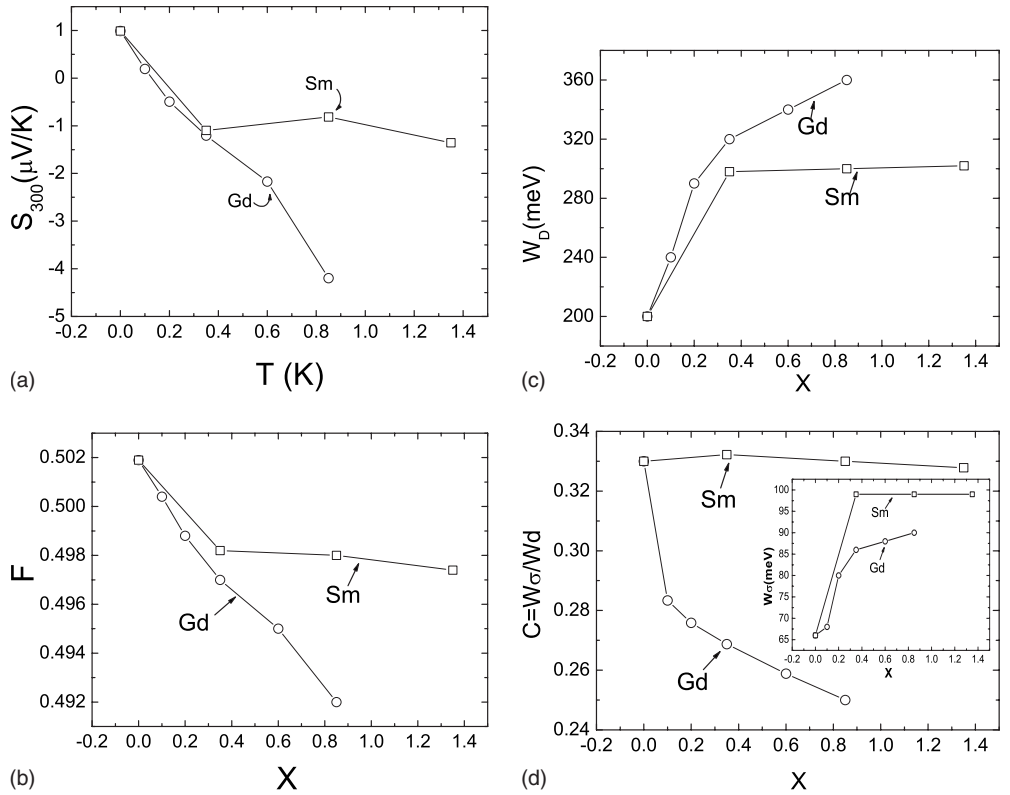

FIG. 3. (a) The concentration dependence of thermopower at 300 K (S_{300}). (b) The concentration dependence of the band filling $F(x)$ of Eq. (1). (c) Concentration dependence of the (density of states) bandwidth. (d) Concentration dependence of the localization parameter $c = w_\sigma / w_D$, and the inset shows the concentration dependence of w_σ.

Sm-doped samples with $x=0.35$ and 1.35 are comparable to that of Gd-doped sample with $x=0.35$. However, $S(T)$'s for $x=0.85$ in the two doped series are quite different from each other, which indicates that the different effect of disorder is presented in the two series. The curves through data in Fig. 2 exemplify fits to a semiempirical model used to analyze our thermopower data. This model suggested by Gasumyants *et al.*[24] is based on the assumption of the narrow band for the charge carriers, and the Fermi energy is located inside a narrow energy interval within which the density of states is larger compared to when it is beyond this interval. Approximate analytical expressions were derived for the temperature dependence of the transport coefficients, and results for $S(T)$ were described in terms of the energy bandwidth for the density of states w_D, the band filling fraction F (the electron concentration divided by the number of states in the band), and the bandwidth w_σ of the effective conductivity $\sigma(\varepsilon)$. So $S(T)$ could be expressed in the following form:

$$S = -\frac{k_B}{e}\left\{\frac{w_\sigma^*}{\sinh w_\sigma^*}\left[e^{-\mu^*} + \cosh w_\sigma^* - \frac{1}{w_\sigma^*}(\cosh \mu^* + \cosh w_\sigma^*)\ln\frac{e^{\mu^*} + e^{w_\sigma^*}}{e^{\mu^*} + e^{-w_\sigma^*}}\right] - \mu^*\right\}. \quad (1)$$

with

$$\mu^* = \frac{\mu}{k_B T} = \ln\frac{\sinh(F w_D^*)}{\sinh[(1-F)w_D^*]},$$

$$w_D^* = \frac{w_D}{2k_B T},$$

and

$$w_\sigma^* = \frac{w_\sigma}{2k_B T}$$

The thermopower at high temperatures ($T > 120$ K) is quite well described by the above formula, as shown with the solid line in Fig. 2, and the fitting parameters will be discussed in the following.

Figure 3 shows the doping concentration dependence of the fitting parameters as well as S at 300 K for the two series. The value of S_{300} increases more quickly for Gd doping than that for Sm doping after $x > 0.35$ as observed in Fig. 3(a). As mentioned in Sec. I, a more pronounced weakening of the metallic state for Gd doping than for Sm doping can be concluded, which may be resulted from the different effect of the localization due to Gd and Sm doping just as mentioned in the following. It is found that the fraction of the electron filling $F(x)$, shown in Fig. 3(b), is decreased from more than half to less than half of the narrow band as the doping concentration is increased for the both series, which indicates that the Fermi surface changes from holelike to electronlike

as the doping increases. It is noted that $F(x)$ is decreased faster for Gd doping than that for Sm doping, suggesting that the band structure of the effective conductivity or the Fermi surface is affected more by Gd doping than by Sm doping. Since the number of the charge carriers is not affected by Gd and Sm substitution for Nd, demonstrated by R_H as shown in Fig. 1, the concentration dependence of $F(x)$ suggests that the band structure of the effective conductivity is changed for both doping. This explanation can be verified by concentration dependence of the fitting parameter w_σ, as shown in the inset of Fig. 3(d).

The dopant concentration dependence of w_D is shown in Fig. 3(c). It increases strongly with x for both doping, which suggests that the density of the charge carriers is reduced for both dopings. The change in these bandwidths with x implies the change in the metallic character. We use the ratio $c=w_\sigma/w_D$ to describe the tendency of localization. It is noted that the increase in w_D is stronger than that in w_σ for Gd doping, and the ratio decreases sharply with the dopant concentration for the Gd doping but nearly keeps constant for Sm doping, as shown in Fig. 3(d), which suggests that the band broadening mainly occurs in the localized region of the bands for Gd doping. The ratio decreases faster for Gd doping than that for Sm doping. It may be related to disorder-driven localization for Gd doping, while for the Sm doping the disorder would be weaker due to the difference in the ionic radius ($Gd^{3+}<Sm^{3+}<Nd^{3+}$).

In order to exhibit the change in the metallic character more directly, the temperature dependences of $S(T)$ against $1/T$ is shown in Fig. 4 for Gd-doped sample with $x=085$, and the corresponding resistivity $\ln\rho$ versus $1/T$ is also included in this figure. The linear behaviors are observed at low temperatures ($T<70$ K), indicating that both the thermopower and resistivity could be described by thermal activationlike conduction at this temperature region. That is to say, both S and ρ at low temperatures follow thermally activated conduction; $\rho(T)=\rho_0\exp(\varepsilon/k_BT)$ and $S(T)=(K_B/e)(\varepsilon/k_BT+A)$. This indicates that a strong localization character appears at low temperatures for this sample. At the same time, no such localization character is observed in heavy Sm-doped samples, and this may be resulted from the fact that the difference in ionic radius is smaller for (Nd,Sm) than that for (Nd,Gd).

Another characteristic feature is that a sharp maximum is observed just above the superconducting temperature T_c for the both doping series, and the temperatures corresponding to this maximum of thermopower is constant for Gd doping and changes with dopant concentration, which could be ascribed to some drag, for example phonon or magnon drag due to the carrier-phonon interaction or carrier-magnon interaction. Such behavior is often observed in other electron-doped system reported in former work,[25] but for the hole-doped system no such a maximum was observed and the temperature dependence of the thermopower could be described completely by formula (1) above the transition temperature, which may be resulted from the fact that the electron-phonon or electron-magnon interaction is stronger in the electron-doped system than in the hole-doped one. However, since our data cannot give out strong evidence to analyze the drag effect further, one needs more systematic

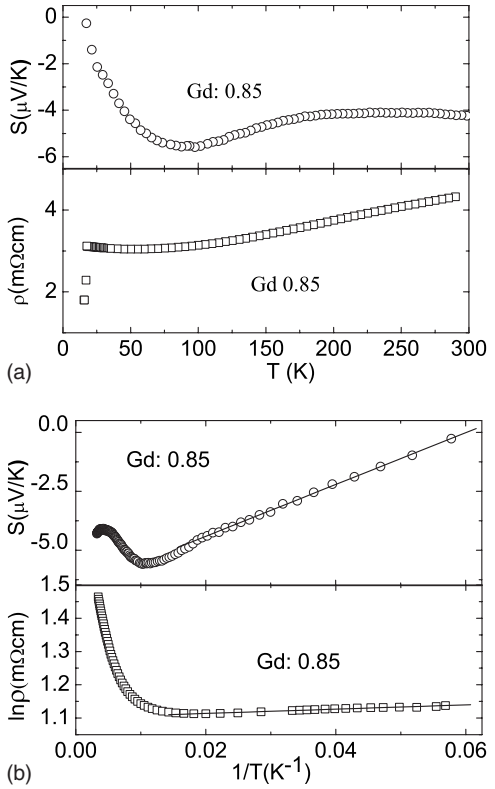

FIG. 4. (a) The temperature dependence of thermopower and *ab*-plane resistivity for $NdGd_{0.85}Ce_{0.15}CuO_{4\pm\delta}$. (b) The plot of S and $\ln\rho$ vs $1/T$ corresponding to (a).

and combined experiments to obtain more information about this. Furthermore, from our thermopower data, we must notice that the useful empirical relation between the magnitude of S at room temperature and the carrier concentration in the planes, just as pointed out by Obertelli *et al.*,[20] is only valid in hole-doped system not in electron-doped system.

In order to clarify the above analysis and the depression of T_c by disorder, the temperature dependence of in-plane resistivity is given out in Fig. 5(a) for the Gd-doped samples and in Fig. 5(b) for the Sm-doped samples, respectively. All the resistivity curves show metallic behavior at high temperatures, and a slight upturn is observed at low temperatures with the increasing doping for both sample series. The transition width ΔT_c estimated from 90% to 10% of the resistance drops is narrow for the samples, which also indicates the high quality of our samples. The normal-state electronic resistivity for the two series increases up to $x=0.85$, but the increase in the resistivity for Gd doping is much stronger than that for Sm doping, which also implies that the localization for samples with Gd doped is induced by electronic disorder just as reported for the hole-doped sample of $R_{1-2x}Ca_xA_xBa_2Cu_3O_{7-\delta}$ (where R is Y, Nd, and Sm and A is Pr or Th.) in Ref. 26. It is also in agreement with the thermopower results that the strong localization would be resulted from the disorder for Gd doping; but for the Sm doping, the disorder-driven localization is weaker due to the smaller difference in ionic radius for (Nd,Sm) than that for (Nd,Gd). The resistivity of the sample with $x=1.35$ is smaller than that with $x=0.85$ for Sm doping, which is easily

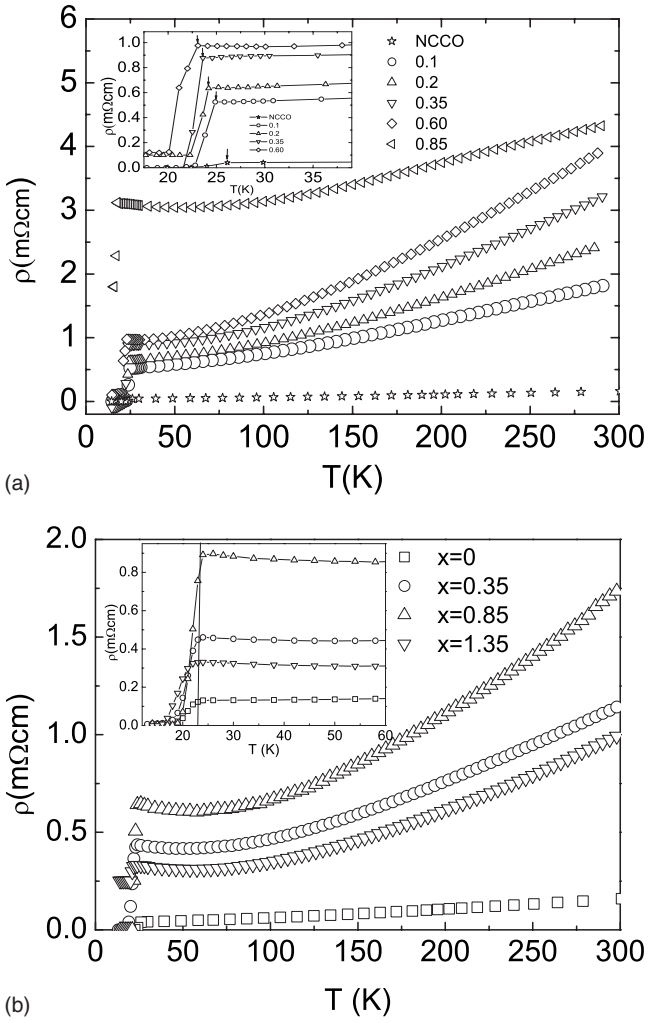

FIG. 5. The temperature dependence of *ab*-plane resistivity ρ for (a) $Nd_{1.85-x}Gd_xCe_{0.15}CuO_{4\pm\delta}$ and (b) $Nd_{1.85-x}Sm_xCe_{0.15}CuO_{4\pm\delta}$ samples. The insets in (a) and (b) show the superconducting transition clearly for each series and the arrow indicates the onset temperature of the superconducting transition.

understood since the compound with $x=0.85$ is the most disordered one among all of the samples we prepared. Furthermore, it is noted that the temperature-independent component ρ_0 (residual resistivity) increases quickly for Gd doping with increasing dopant concentration. This behavior is qualitatively similar to the in-plane resistivity for Zn-substituted single crystals of $YBa_2Cu_3O_{7-y}$ and $La_{2-x}Sr_xCuO_4$ (LSCO),[27] but the magnitude of ρ_0 is much larger. It is found that ρ_0 increases slightly before x reaches 0.85 and then decreases with further doping. This phenomenon indicates that the scattering mechanisms are different among Zn-, Gd-, and Sm-doped systems. It is known that residual resistivity is a measure of the scattering rate of the charge carriers by impurities or defects in a crystal. It is interesting to make a comparison with the result for Zn-doped samples, but since no reports about Zn-substituted single crystals of the electron-doped system were observed up to now, we could only compare our results with the conclusions of the hole-doped $La_{1.85}Sr_{0.15}Cu_{1-z}Zn_zO_4$ compound.[27] In the following paragraph we will emphasize on the depression of the T_c, the

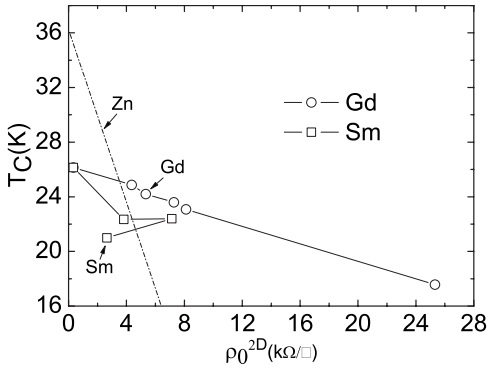

FIG. 6. T_c vs disorder-induced ρ_0^{2D}. The dotted curves connecting the data are guides for the eyes. For comparison, the result for the Zn-doped LSCO with $x=0.15$ is shown by the dashed curve (Ref. 27).

increase in the residual resistivity ρ_0, and their relation.

As pointed out in Ref. 27, ρ_0 increases more strongly for Zn-doped system into Cu sites than that for *M* introduced into the building block in hole-doped $La_{1.85}Sr_{0.15}CuO_4$ system. That is to say, the impurity Zn doping is strong carrier scattering, while the substituted *M* works as weak elastic scatterings. But in our case, ρ_0 increases much more strongly for Gd introduced into the building block than Zn doping in $La_{1.85}Sr_{0.15}CuO_4$, which indicates that the substituted Gd works as stronger scattering. The present result is not in agreement with that reported in Ref. 27, and it may be suggestive of a novel effect of the disorder, which is not understood in detail. Moreover, in the case of Zn doping for $La_{1.85}Sr_{0.15}CuO_4$, a universal relation between T_c reduction and residual resistivity is obtained, and T_c goes to 0 as Zn-induced ρ_0^{2D} (two-dimensional residual resistivity per CuO_2 plane) approaches the value near the two-dimensional universal resistance $h/4e^2$ (about 6.5 kΩ/□) at which a superconductor-insulator transition takes place. Based on these observations, a phase-fluctuation scenario was proposed by Emery and Kivelson[28] to explain the T_c reduction mechanism due to Zn. However, for Gd-substituted $Nd_{1.85-x}Gd_xCe_{0.15}CuO_{4\pm\delta}$, we do not find the superconductor-insulator transition as ρ_0^{2D} increases beyond the critical value $h/4e^2$ but observe the coexistence of the superconductivity and localization just as presented in Figs. 3(a) and 3(b), which is in agreement with the result of the infrared conductivity of $Y_{1-x}Pr_xBa_2Cu_3O_7$ films where the coexistence of the superconductivity and localization was also observed in the hole-doped system.[29] To make a quantitative comparison, T_c is plotted against ρ_0^{2D} for the present systems in Fig. 6, together with the data for the Zn-substituted $La_{1.85}Sr_{0.15}CuO_4$ shown by the dashed line.[27] One can immediately see that the disorder outside the CuO_2 planes for Gd doping does not reduce T_c as much as the Zn doping does for the hole-doped system even though it induces much larger ρ_0^{2D}, suggesting that the mechanism of the T_c reduction due to disorder outside the CuO_2 planes for the electron-doped system is different from that due to Zn doping for the hole-doped system. But for the Sm doping, T_c nearly remains constant, which implies that Sm and Gd doping also have different impact on T_c. These observations sug-

gest that T_c of Gd-doped samples is depressed due to electronic disorder according to the resistivity, while for Sm-doped samples other mechanisms would seem to dominate. To further investigate this idea we now compare the results in Fig. 6 with conventional disorder theories. Quantum corrections to T_c due to disorder have been calculated for BCS-type superconductors by Fukuyama *et al.*[30] as a function of a disorder parameter $\hbar/\varepsilon_F\tau$. ε_F is the Fermi energy and τ is the elastic relaxation time. $\hbar/\varepsilon_F\tau$ is closely related to the resistivity ρ and is usually replaced with ρ in work where experiments are compared with this theory. For example, it has been shown that Fukuyama-Ebisawa-Maekawa (FEM) theory can account well for the depression of T_c in a large number of superconductors where disorder had been varied by different means.[31] So the depression of T_c could be qualitatively explained by quantum interference effects for Gd doping but not for Sm doping just as reported for the hole-doped sample $R_{1-2x}Ca_xA_xBa_2Cu_3O_{7-\delta}$ in Ref. 26. It might be possible that a larger resistivity for Gd arises from the smaller ionic radius. At the same time, in the present results of $S(x,T)$, it is found from Fig. 3(d) that the ratio w_σ/w_D is decreased monotonously with increasing x for Gd doping, but almost constant for Sm doping, whose tendency is similar to the tendency of the doping concentration dependence of T_c. This implies that the depression of T_c may be mainly dominated by the localization and the change in the band structure, and $S(x,T)$ also implies that the broadening of the bands and the increasing localization for Gd doping qualitatively support a decrease in both τ and ε_F with increasing x, which also confirms and supplements the picture reported in Ref. 26.

IV. SUMMARY

The normal-state thermoelectric power, Hall-effect, and resistivity experiments were performed on $Nd_{1.85-x}M_xCe_{0.15}CuO_{4\pm\delta}$ (M=Gd and Sm) single crystals with different doping concentration. The thermopower above 120 K is analyzed on the basis of a semiempirical model with three free parameters describing characteristic features of the band structure. Good descriptions of $S(T)$ were obtained in this model for each alloy system. A consistent doping concentration dependence of corresponding parameters was obtained in this model. Both the energy bandwidth for the density of states w_D and the bandwidth w_σ of the effective conductivity $\sigma(\varepsilon)$ increase for increasing Gd and Sm doping, but the band filling fraction $F(x)$ is decreased. The ratio w_σ/w_D decreases with x for Gd doping, but it is nearly constant for Sm doping which, together with a stronger increase in the electrical resistivity for Gd doping, indicates that the localization tendency is driven by electronic disorder for this doping. For Sm doping the results suggest a weaker disorder effect, which may be resulted from the difference in ionic radius. Moreover, for Gd doping the superconducting T_c is strongly depressed with increasing the doping concentration, while for Sm doping T_c is nearly unchanged with increasing Sm content, which indicates that the superconducting T_c may be related to the localization and the band structure of the itinerant carriers.

ACKNOWLEDGMENTS

Financial support from the National Natural Science Foundation of China (Grant No. 10374082) is gratefully acknowledged.

*Corresponding author. Present address: Physics Dept., University of Science and Technology of China, Hefei, Anhui, P. R. China 230026. Fax: +86-551-3601073; yanghs@ustc.edu.cn

[1] H. Eisaki, N. Kaneko, D. L. Feng, A. Damascelli, P. K. Mang, K. M. Shen, Z. X. Shen, and M. Greven, Phys. Rev. B **69**, 064512 (2004).
[2] Y. Onose, Y. Taguchi, K. Ishizaka, and Y. Tokura, Phys. Rev. Lett. **87**, 217001 (2001).
[3] J. L. García-Muñoz, M. Suaaidi, J. Fontcuberta, S. Piñol, and X. Obradors, Physica C **268**, 173 (1996).
[4] P. K. Mang, S. Larochelle, A. Mehta, O. P. Vajk, A. S. Erickson, L. Lu, W. J. L. Buyers, A. F. Marshall, K. Prokes, and M. Greven, Phys. Rev. B **70**, 094507 (2004).
[5] H. Wu, L. Zhao, J. Yuan, L. X. Cao, J. P. Zhong, L. J. Gao, B. Xu, P. C. Dai, B. Y. Zhu, X. G. Qiu, and B. R. Zhao, Phys. Rev. B **73**, 104512 (2006).
[6] R. C. Budhani, M. C. Sullivan, C. J. Lobb, and R. L. Greene, Phys. Rev. B **66**, 052506 (2002).
[7] H. X. Gao, H. S. Yang, Y. S. Chai, J. Liu, C. H. Sun, L. Cheng, J. B. Wang, and L. Z. Cao, Phys. Lett. A **369**, 493 (2007); C. H. Sun, H. S. Yang, L. Cheng, J. B. Wang, and L. Z. Cao, Supercond. Sci. Technol. **21**, 085018 (2008).
[8] R. C. Budhani, M. C. Sullivan, C. J. Lobb, and R. L. Greene, Phys. Rev. B **65**, 100517(R) (2002).
[9] X. Zhao, X. F. Sun, L. Wang, W. B. Wu, and X. G. Li, J. Phys.: Condens. Matter **13**, 4303 (2001).
[10] S. R. Ghorbani, M. Andersson, and Ö. Rapp, Phys. Rev. B **66**, 104519 (2002).
[11] J.-S. Zhou, J. P. Zhou, J. B. Goodenough, and J. T. McDevitt, Phys. Rev. B **51**, 3250 (1995).
[12] C. Bernhard and J. L. Tallon, Phys. Rev. B **54**, 10201 (1996).
[13] J. L. Tallon, J. R. Cooper, P. S. I. P. N. de Silva, G. V. M. Williams, and J. W. Loram, Phys. Rev. Lett. **75**, 4114 (1995).
[14] J. W. Cochrane, G. J. Russel, and D. N. Matthews, Physica C **232**, 89 (1994).
[15] G. V. M. Williams, M. Staines, J. L. Tallon, and R. Meinhold, Physica C **258**, 273 (1996).
[16] D. Mandrus, L. Forro, C. Kendziora, and L. Mihaly, Phys. Rev. B **44**, 2418 (1991).
[17] X. H. Chen, T. F. Li, M. Yu, K. Q. Ruan, C. Y. Wang, and L. Z. Cao, Physica C **290**, 317 (1997).
[18] R. Wang, H. Sekine, and H. Jin, Supercond. Sci. Technol. **9**, 529 (1996).
[19] M. Y. Choi and J. S. Kim, Phys. Rev. B **59**, 192 (1999).
[20] S. D. Obertelli, J. R. Cooper, and J. L. Tallon, Phys. Rev. B **46**, 14928 (1992).

[21] M. Brinkman, T. Rex, M. Stief, H. Bach, and K. Westerhalt, Physica C **269**, 76 (1996).
[22] W. Jiang, X. Q. Xu, S. J. Hagen, J. L. Peng, Z. Y. Li, and R. L. Greene, J. Supercond. **7**, 773 (1994).
[23] C. H. Wang, L. Huang, L. Wang, Y. Peng, X. G. Luo, Y. M. Xiong, and X. H. Chen, Supercond. Sci. Technol. **17**, 469 (2004).
[24] V. E. Gasumyants, V. I. Kadanov, and E. V. Vladimirskaya, Physica C **248**, 255 (1995).
[25] H. S. Yang, Y. S. Chai, J. Liu, M. Yu, P. C. Li, L. Zhang, M. D. Li, and L. Z. Cao, Physica C **403**, 203 (2004).
[26] B. Lundqvist, P. Lundqvist, and Ö. Rapp, Phys. Rev. B **57**, 14428 (1998).
[27] Y. Fukuzumi, K. Mizuhashi, K. Takenaka, and S. Uchida, Phys. Rev. Lett. **76**, 684 (1996).
[28] V. J. Emery and S. A. Kivelson, Phys. Rev. Lett. **74**, 3253 (1995).
[29] R. P. S. M. Lobo, E. Ya. Sherman, D. Racah, Y. Dagan, and N. Bontemps, Phys. Rev. B **65**, 104509 (2002).
[30] H. Fukuyama, H. Ebisawa, and S. Maekawa, J. Phys. Soc. Jpn. **53**, 3560 (1984); **53**, 1919 (1984).
[31] M. Ahlgren, P. Lindqvist, A. Nordström, and Ö. Rapp, Phys. Rev. B **49**, 9716 (1994).